Unbound excited states of the N=16 closed shell nucleus ^{24}O

W. F. Rogers *et al.*

Phys. Rev. C **92**, 034316 — Published 16 September 2015

DOI: 10.1103/PhysRevC.92.034316

Unbound excited states of the N=16 closed shell nucleus ^{24}O

W.F. Rogers,[1,*] S. Garrett,[1] A. Grovom,[1] R.E. Anthony,[2] A. Aulie,[1] A. Barker,[1] T. Baumann,[3] J.J. Brett,[4] J. Brown,[5] G. Christian,[3,6,†] P.A. DeYoung,[4] J.E. Finck,[7] N. Frank,[8] A. Hamann,[1] R.A. Haring-Kaye,[2] J. Hinnefeld,[9] A.R. Howe,[2] N.T. Islam,[2] M.D. Jones,[3,6] A.N. Kuchera,[3,6] J. Kwiatkowski,[1] E.M. Lunderberg,[4,‡] B. Luther,[10,§] D.A. Meyer,[11] S. Mosby,[3,6,¶] A. Palmisano,[12,‡] R. Parkhurst,[1] A. Peters,[12] J. Smith,[3,6,†] J. Snyder,[3,6] A. Spyrou,[3,6] S.L. Stephenson,[12] M. Strongman,[3,6,**] B. Sutherland,[1] N.E. Taylor,[1] and M. Thoennessen[3,6]

[1]*Department of Physics, Westmont College, Santa Barbara CA 93108*
[2]*Department of Physics and Astronomy, Ohio Wesleyan University, Delaware OH 43015*
[3]*National Superconducting Cyclotron Laboratory, Michigan State University, East Lansing MI 48824*
[4]*Department of Physics, Hope College, Holland MI 49422*
[5]*Department of Physics, Wabash College, Crawfordsville IN 47933*
[6]*Department of Physics and Astronomy, Michigan State University, East Lansing MI 48824*
[7]*Department of Physics, Central Michigan University, Mount Pleasant MI 48859*
[8]*Department of Physics and Astronomy, Augustana College, Rock Island IL 61201*
[9]*Department of Physics and Astronomy, Indiana University, South Bend IN 43364*
[10]*Department of Physics, Concordia College, Moorhead MN 56562*
[11]*Department of Physics, Rhodes College, Memphis TN 38112*
[12]*Department of Physics, Gettysburg College, Gettysburg PA 17325*

Two low-lying neutron-unbound excited states of ^{24}O, populated by proton-knockout reactions on ^{26}F, have been measured using the MoNA and LISA arrays in combination with the Sweeper Magnet at the Coupled Cyclotron Facility at the NSCL using invariant mass spectroscopy. The current measurement confirms for the first time the separate identity of two states with decay energies 0.51(5) MeV and 1.20(7) MeV, and provides support for theoretical model calculations, which predict a 2^+ first excited state and a 1^+ higher energy state. The measured excitation energies for these states, 4.70(15) MeV for the 2^+ level and 5.39(16) MeV for the (1^+) level, are consistent with previous lower-resolution measurements, and are compared with five recent model predictions.

I. INTRODUCTION

The study of nuclear structure near the neutron dripline has received much attention in recent years, aided by the increasing availability of rare isotope beams. Observed changes in nuclear shell structure far removed from the line of stability have provided important data for testing theoretical models. The disappearance of magic numbers 8 and 20 far from stability were observed, for example, in the low excitation energy and large quadrupole transition rates for the first 2^+ states in ^{12}Be [1] and ^{32}Mg [2], while the appearance of a relatively large shell gap at $N = 16$ was suggested [3–6] and first observed in a survey of neutron separation energies [7]. The lack of particle-bound excited states in ^{24}O [8], the measured decay energy of the unbound ground state of ^{25}O [9], and the determination of the neutron occupancies extracted from the single neutron removal reaction from ^{24}O [10, 11] support this conclusion.

An additional signature for shell closure is a marked drop in nuclear collectivity, evidenced by a high energy for the first excited state. The two lowest neutron-unbound excited states in ^{24}O were measured using a proton-knockout reaction on ^{26}F [12]. The first excited 2^+ state was found to have an energy of $E_x = 4.72(11)$ MeV, providing strong support for the $N = 16$ shell closure and establishing ^{24}O as a doubly magic nucleus. The shape and the large width of the observed peak led to an interpretation based on two components with the upper resonance corresponding to the (presumed) 1^+ level at an excitation energy of 5.33(12) MeV. This interpretation was guided by various theoretical calculations [3–5, 13, 14] which predict a doublet of excited states having spin/parity assignments $I^\pi = 2^+$ and 1^+ with the 1^+ being higher in energy. These two states should be dominated by the $1s_{1/2} \times 0d_{3/2}$ configuration. A subsequent experiment using inelastic proton scattering from ^{24}O at RIKEN [15] also observed a broad unresolved peak consistent with the earlier results. The peak was again analyzed with two components where a measurement of the angular distribution provided confirmation for a 2^+ spin/parity assignment for the lower resonance [15]. Although theoretically two resonances are expected and both experiments indicate their presence, the two states remained largely unresolved. Thus a main goal in the current experiment was to obtain an clear separation between the two ^{24}O neutron-unbound

* rogers@westmont.edu
† Present address: TRIUMF, Vancouver, British Columbia, V6T2A3, Canada
‡ Present address: National Superconducting Cyclotron Laboratory, Michigan State University, East Lansing MI 48824; Department of Physics and Astronomy, Michigan State University, East Lansing MI 48824
§ Present address: St. John's College, Annapolis MD 21401
¶ Present address: Los Alamos National Laboratory (LANL), Los Alamos NM 87545
** Present address: Air Force Technical Applications Center, Patrick AFB, FL 32925

excited states by using a thinner target than in the previous NSCL experiment.

II. EXPERIMENT

The experiment was performed at the National Superconducting Cyclotron Laboratory (NSCL) at Michigan State University. A 76 MeV/u ^{26}F secondary beam was produced by the Coupled-Cyclotron Facility from the fragmentation of a 140 MeV/u ^{48}Ca beam on a 987 mg/cm^2 Be production target. The A1900 Fragment Separator [16] was tuned to select the ^{26}F fragments and a 1050 mg/cm^2 Al wedge was located at its intermediate focal plane to reduce contaminants.

The ^{26}F beam rate was 1.2 pps/pnA with a momentum acceptance $\Delta p/p = 1\%$ and a beam purity of 3.3%. The majority of the remaining beam consisted of contaminant ^{29}Na fragments. The ^{26}F beam particles were identified and separated from the other contaminant components during the analysis by time-of-flight. The secondary beam was directed onto a 188 mg/cm^2 Be target. Low-lying excited states of ^{24}O are likely populated either by the knockout of a p-shell proton in ^{26}F followed by neutron emission from the continuum or by direct removal of a valence proton together with a neutron [12]. These processes are indistinguishable with the present experimental setup.

Charged fragments emerging from the secondary Be target were deflected out of the beam path by a large-gap superconducting dipole Sweeper Magnet [17] set to a central track rigidity of 3.714 Tm, and directed into the Sweeper detector chamber. Trajectories of the charged fragments were determined using the two Cathode Readout Drift Chamber (CRDC) detectors, and the fragment energy and energy loss were determined using an ion chamber and thin and thick plastic scintillators. The ^{23}O fragments resulting from the ^{24}O unbound excited state decays were separated from all other fragments using their specific trajectory and time-of-flight characteristics.

Neutrons were detected with the Modular Neutron Array (MoNA) [18] and the Large-area multi-Institutional Scintillator Array (LISA). Each array consists of 144 2.0 m $\times$ 0.10 m $\times$ 0.10 m plastic scintillator bars with photomultiplier tubes attached to each end for position sensitivity along their length. The current experiment served as the commissioning run for LISA. The addition of LISA results in wider angular coverage and hence greater neutron detection efficiency for the system. This increased efficiency along with the higher available beam-rates allowed for use of a target 2.5 times thinner than in the previous NSCL experiment. Target thickness is typically the dominant contributor to the overall decay energy resolution for invariant mass spectroscopy experiments, and neutron angle resolution begins to dominate the resolution as the target becomes very thin.

The current experiment is essentially identical to the measurement by Hoffman *et al.* [12] but with higher resolution, since we used a target 2.5 times thinner and included the LISA array. The energy-dependent resolution for the current measurement was determined through Monte Carlo simulation to be $18\sqrt{E_{decay}(\mathrm{keV})}-24(\mathrm{keV})$, which includes experimental factors such as target thickness (typically a dominant contributor to overall resolution) and detector acceptances and efficiencies. Unfortunately, due to a malfunction of the tracking detectors only a total of approximately 170 ^{23}O-neutron coincidence events were collected. Since ^{23}O has no particle-bound excited states [8], the detection of fragment-neutron coincidences sufficed to identify the ^{24}O decays uniquely.

III. DATA ANALYSIS

For the determination of the neutron decay energy, kinematics of both the fragment and the neutron (direction and energy) are necessary at the site of the decay within the secondary target. Since all fragment trajectories and energies are determined after passage through the Sweeper Magnet, an inverse tracking matrix technique was used to reconstruct the momentum and energy of the fragments at the target from the measured values behind the magnet [19]. The neutron kinematics were determined from the position of the first neutron interaction in MoNA and LISA and the time-of-flight from the secondary target to the arrays.

The ^{24}O decay energy spectrum ($E_{decay} = M_{^{24}O} - M_f - M_n$) was then reconstructed from the invariant mass which uses the total energies (E_f, E_n) and momenta (p_f, p_n) of the fragment and the neutron, as well as the angle between their decay trajectories θ_{fn}, all measured in the lab frame:

$$M_{^{24}O} = \sqrt{M_f^2 + M_n^2 + 2\left(E_f E_n - p_f p_n \cos\theta_{fn}\right)} \quad (1)$$

where m_f and m_n are the rest masses of the ^{23}O fragment and neutron. Figure 1 shows the decay energy spectrum for the 170 ^{23}O-neutron coincidences. The overall spectrum agrees with the previous MoNA data. In spite of the limited statistics a separate peak near 1 MeV is visible in addition to the low energy peak around 500 keV.

In order to extract resonance energies and widths Monte Carlo simulations were performed. Resonance decay peaks were modeled using energy-dependent Breit-Wigner line-shapes as prescribed by the R-matrix formulation [20] and guided by the results of the previous measurements and shell model calculations. The lower level has a confirmed spin-parity $I^\pi = 2^+$ [15], which decays to the ^{23}O $1/2^+$ ground state via an $l = 2$ neutron. The upper level is presumed to have spin-parity assignment of 1^+, though that has not yet been experimentally confirmed. For the ^{24}O 1^+ excited state neutron decay to the $1/2^+$ ^{23}O ground state, the USD shell model calculation [24] predicts a spectroscopic factor of zero for the $l = 0$ decay and about 0.9 for the $l = 2$ decay. Both

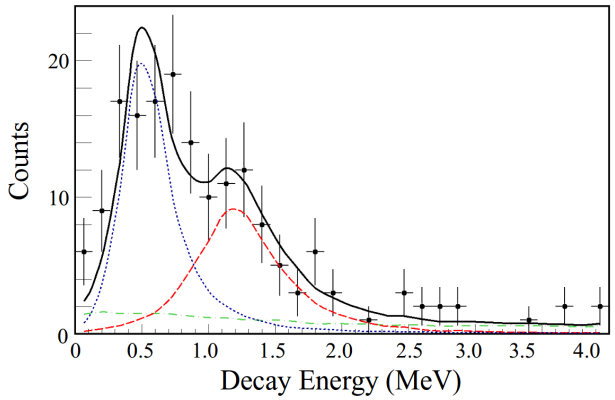

FIG. 1. (color online) Decay energy spectrum of ^{24}O. The experimental data are not corrected for detector acceptances and efficiencies. The data were fit with two asymmetric Breit-Wigner resonances (blue dot and red dash curves) and a non-resonant background (green dash-dot curve) determined through Monte-Carlo simulation and χ^2 minimization.

peaks were therefore modeled using $l = 2$ neutron decays. Each Breit-Wigner line shape was then used as input to a Monte Carlo calculation that included features of the experimental arrangement, including target energy loss and straggling, a Glauber model for the nuclear reaction, and the Sweeper chamber and neutron detector acceptances and efficiencies. Simulated resonances for each of the two peaks were produced with several different energies and widths which then allowed a global χ^2 minimization procedure to determine which resonance parameters best fit the experimental spectrum. The non-resonant portion of the spectrum arising from ^{25}O neutrons was modeled using a Gaussian energy distribution with a peak energy of 15 MeV with $\sigma = 7.5$ Mev.

A global minimization of χ^2 for a variety of energies, scaling factors, widths, and non-resonant neutron temperatures resulted in best-fit decay energies 0.51 ± 0.05 MeV and 1.20 ± 0.07 MeV, with widths $\Gamma = 0.04^{+0.01}_{-0.04}$ MeV and $0.16^{+0.08}_{-0.16}$ MeV for the 2^+ and (1^+) states, respectively. The lower limits on the width uncertainties reflect consistency with $\Gamma = 0$ within the 1σ limit, and the upper limits correspond to single particle widths for the two transitions, each within the 1σ limit, which are $\Gamma_{sp} = 0.05$ MeV and $\Gamma_{sp} = 0.22$ MeV, respectively [21]. The best fit for the data are shown in Figure 1.

The energy levels for the 2^+ and (1^+) states are computed by adding the ^{24}O 1-n separation energy S_n, corresponding to the mass difference between ^{24}O and ^{23}O, to the measured decay energies. Using the separation energy for ^{24}O adopted from the newest AME2012 Atomic Mass Evaluation table [22], $S_n = 4.19(14)$ MeV, the energies for the two excited states are then $E_{2^+} = 4.70(15)$ MeV and $E_{1^+} = 5.39(16)$ MeV. Note that the previous NSCL and RIKEN experiments each used a separation energy $S_n = 4.09(10)$ MeV suggested by Jurado *et al.* [23] in 2007, which is 100 keV lower than the more current AME2012 value.

IV. RESULTS AND DISCUSSION

Figure 2 compares the current 2^+ and (1^+) level decay energy values with the two previous measurements at NSCL (0.63(4) MeV and 1.24(7) MeV, respectively) [12] and RIKEN (0.56(7) MeV and 1.06(11) MeV, respectively) [15] . The data are fairly consistent with one another.

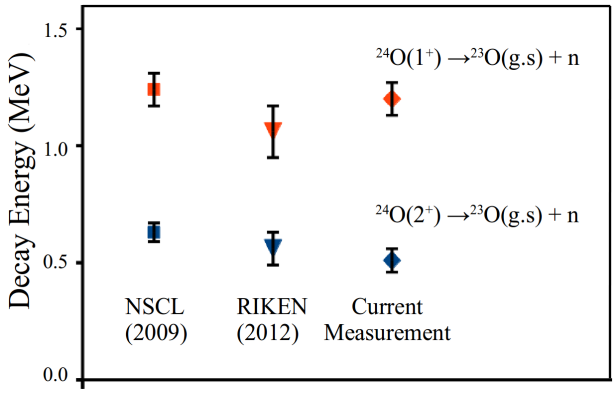

FIG. 2. (color online) Measured decay energies for the ^{24}O(2^+) →^{23}O(g.s) + n (lower blue points) and the ^{24}O(1^+) →^{23}O(g.s) + n (upper red points) neutron decays. Current measurements (diamond) and the previous NSCL (square) [12] and RIKEN (triangle) [15] results are shown. The current results are generally consistent with the two previous measurements.

A comparison of the ^{24}O 2^+ and (1^+) level energies for the three different experiments is shown in Figure 3. For consistency, the levels for all three experiments are computed using the same (latest) ^{24}O neutron separation energy $S_n = 4.19(14)$ MeV [22]. As mentioned in the previous section, both Hoffman and Tshoo used an earlier value of $S_n = 4.09(10)$ MeV [23] so that their energies appear approximately 100 keV higher in this figure than in the original papers.

It is interesting to note the different degrees of internal agreement for Figures 2 and 3. The error bars for the decay energy data shown in Figure 2 have relatively low overlap, the largest difference being nearly 2σ between the 2009 and current NSCL/MoNA measurements of the lower state decay. The error bars for the excited state level energies shown in Figure 3 have more substantial overlap because the uncertainties in the mass measurements (needed for the energy level computations) are larger than those in the decay energies. Figure 4 shows the evolution of ^{24}O and ^{23}O mass measurements over time. Of particular note is the wide variation of the ^{24}O mass, where the recommended value has changed by over 500 keV. High resolution mass measurements of ^{24}O and ^{23}O would be very valuable in order to further reduce the uncertainty in excitation energies for neutron unbound states.

In Figure 3 the ^{24}O excited state energy levels for the current and previous measurements are compared with four of the most recent theoretical calculations as well as with USD, USD-05A, and USD-05B shell model calculations [24]. The four recent analyses are based on 1)

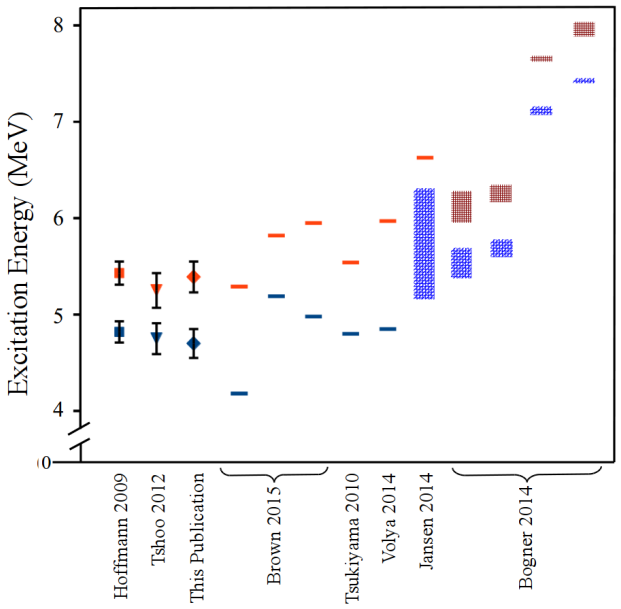

FIG. 3. (color online) A comparison of the measured 2^+ (lower blue) and (1^+) (upper red) energy levels in ^{24}O (including those from Hoffmann 2009 [12] and Tshoo 2012 [15] adjusted for the separation energy S_n used in this paper [22]) Included also are predictions from Brown 2015 (left to right: USD, USD-05A and USD-05B) [24], Tsukiyama 2010 CCSM [14], and Volya 2014 CSM [25] shell model calculations, as well as *ab initio* calculations from Jansen 2014 CCEI model [26], and Bogner 2014 IM-SRG model (left to right: $\Lambda_{3N} = 400, 400, 500, 500$ MeV and $\lambda_{SRG} = 1.88, 2.24, 1.88, 2.24$ fm^{-1}, respectively) [27]. Hatched regions correspond to level energy ranges reported in the original citations.

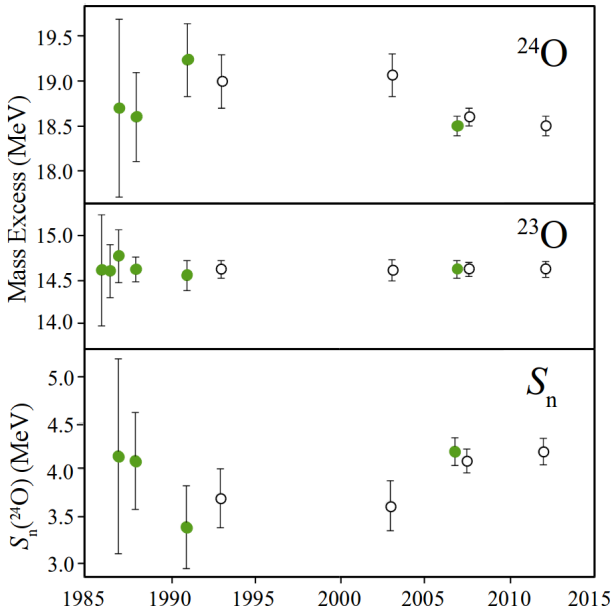

FIG. 4. (color online) Evolution of the ^{23}O and ^{24}O mass measurements over time. Experimental determinations (solid circles) of the ^{24}O and ^{23}O mass measurements, as well as the 1-n separation energies S_n are shown along with the AME recommended values (open circles). Measurement values are from references [23, 28–32] and the recommended values are from references [22, 23, 33, 34].

a continuum-coupled shell model (CCSM) which extends the normal shell model to include continuum states [14], 2) a continuum shell model (CSM) based on an effective non-Hermitian Hamiltonian [25], 3) an *ab initio* coupled cluster effective shell model interaction (CCEI) [26], and 4) an *ab initio* construction of valence-space Hamiltonians based on chiral two- and three-body nucleon interactions using the in-medium similarity renormalization group (IM-SRG) [27]. For the IM-SRG results, Λ_{3N} values denote cutoffs for the 3N interaction in MeV, and λ_{SRG} values denote momentum resolution scales in fm^{-1}.

Of the model predictions included for this comparison, the phenomenological CCSM model [14] reproduces the data best, with the USD [3, 4, 24] and CSM model calculations [25] next best; the USD model under-predicts the state energies by about the same amount as the CSM over-predicts them. While both the CCEI [26] and the IM-SRG [27] calculations over-predict the energies of the two levels, the level of agreement is, nevertheless, impressive given that these calculations are from first principle. Of these, the CCEI calculation and the IM-SRG calculation with a $\Lambda_{3N} = 400$ MeV interaction cutoff yield best agreement with experimental data.

Figure 5 plots the difference in energy between the (1^+) and 2^+ states for the same data and model predictions. The USD-05A and CCSM model predictions reproduce the energy level difference quite well. The *ab initio* model predictions yield better agreement with the data than do the USD, USD05B and CSM model predictions, which over-predict the energy splitting by almost a factor of 2.

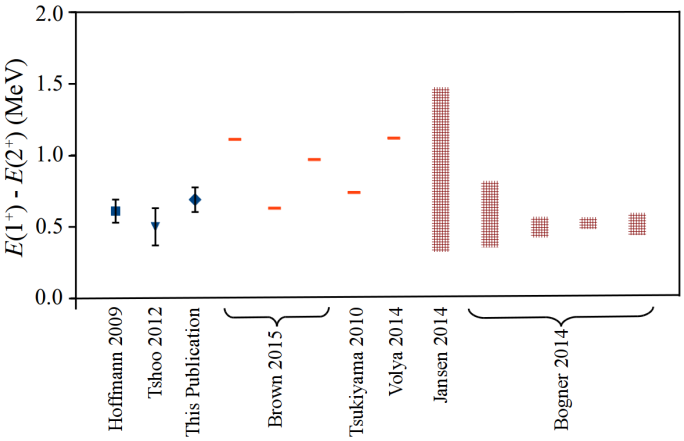

FIG. 5. (color online) Difference in energy between the 1^+ and 2^+ states in ^{24}O for the three measurements (blue) and values from theory (red). References are the same as those described in Figure 3.

V. CONCLUSION

We report a new measurement of the energies of the first two excited states in neutron-rich ^{24}O. The new

Large-area multi-Institutional Scintillator Array (LISA) was successfully commissioned. The overall increase in neutron detection efficiency and higher available beam rates allowed the use of a thinner target, improving experimental resolution over previous measurements and allowing the states to be cleanly resolved for the first time. The newly extracted excitation energy values of 4.70(15) MeV and 5.39(16) MeV are consistent with two earlier measurements. The level energy uncertainties are dominated by ^{24}O mass measurement uncertainty and not by the precision of the decay energy measurements. Thus a high resolution mass measurement is required to increase the precision of the experimental results for comparison with theory. Such measurements are already within reach of state of the art penning trap systems, for example TITAN at TRIUMF [35, 36]. However, these measurements await the development of very neutron rich, low-energy oxygen beams at the corresponding radioactive beam facilities.

VI. ACKNOWLEDGEMENTS

We would like to thank the operations staff at NSCL for providing the primary ^{48}Ca and secondary ^{26}F beams for this experiment. WFR would like to thank B.A. Brown for helpful conversations. This work is supported by NSF grants PHY-0922335, PHY-0922409, PHY-0922446, PHY-0922462, PHY-0922473, PHY-0922537, PHY-0922559, PHY-0922622, PHY-0922794, PHY-0969173, PHY-1101745, PHY-1205357, PHY-1205537. This work is also based upon work supported by the Department of Energy National Nuclear Security Administration under Award No. DE-NA0000979.

[1] H. Iwasaki *et al.*, Phys. Lett B **481** 7 (2000)
[2] T. Motobayashi *et al.*, Phys. Let B **346** 9 (1995)
[3] B.A. Brown, B.H. Wildenthal, Ann. Rev. Part. Nucl. Sci. **38** 29 (1988)
[4] B.A. Brown, W.A. Richter, Phys. Rev. C **74** 034315 (2006)
[5] Y. Utsuno, T. Otsuka, T. Mizusaki, and M. Honma, Phys. Rev. C **60** 054315 (1999)
[6] T. Otsuka *et al.*, Phys Rev. Lett. **87** 082502 (2001)
[7] A. Ozawa, T. Kobayashi, T. Suzuki, K. Yoshida, and I. Tanihata, Phys. Rev. Lett. **84** 5493 (2000)
[8] M. Stanoiu *et al.*, Phys. Rev C **69** 034312 (2004)
[9] C.R. Hoffman *et al.*, Phys. Rev. Lett. **100** 152502 (2008)
[10] R. Kanungo *et al.*, Phys. Rev. Lett. **102**, 152501 (2009)
[11] K. Tshoo *et al.*, Phys. Lett. B **739**, 19 (2014)
[12] C.R. Hoffman *et al.*, Phys. Lett. B **672** 17 (2009)
[13] A. Volya, V. Zelevinsky, Phys. Rev. Lett. **94** 052501 (2005)
[14] K. Tsukiyama, T. Otsuka, R. Fujimoto, arXiv:1001.0729 (2010)
[15] K. Tshoo *et al.*, Phys. Rev. Lett. **109** 022501 (2012)
[16] D.J. Morrissey *et al.*, Nucl. Instrum. Meth. B **204**, 90 (2003)
[17] M.D. Bird *et al.*, IEEE Trans. Appl Supercond. **15** 1252 (2005)
[18] T. Baumann *et al.*, Nucl. Instrm Meth. A **543** 517 (2005)
[19] N. Frank *et al.*, Nucl. Instr. Meth. A **580** 1478 (2007)
[20] A.M. Lane, R.G. Thomas, Rev. Mod. Phys. **30** 257 (1958)
[21] A. Bohr and B.R. Mottelson, Nuclear Structure Vol. 1, World Scientific Publishing Co. Pte. Ltd., 1998, p.441
[22] Wang *et al.*, Chinese Phys. C **36** 1603 (2012)
[23] B. Jurado *et al.*, Phys. Lett. B **649** 43 (2007)
[24] B.A. Brown, https://people.nscl.msu.edu/∼brown/resources/resources.html (2015)
[25] A. Volya and V. Zelevinsky, Phys. of Atom. Nucl. **77** 969 (2014)
[26] G.R. Jansen, J. Engel, G. Hagen, P. Navratil, and A. Signoracci, Phys Rev. Lett. **113** 142502 (2014)
[27] S.K. Bogner *et al.*, Phys. Rev. Lett. **113** 142501 (2014)
[28] A. Gillibert *et al.*, Phys. Lett. B **176** 317 (1986)
[29] D.J. Vieira *et al.*, Phys. Rev. Lett. **57** 3253 (1986)
[30] A. Gillibert *et al.*, Phys. Lett. B **192** 39 (1987)
[31] J.M. Wouters *et al.*, Z. Phys. **A331** 229 (1988)
[32] N.A. Orr *et al.*, Phys. Lett B **258** 29 (1991)
[33] G. Audi *et al.*, Nucl. Phys. A **595** 409 (1995)
[34] G. Audi *et al.*, Nucl. Phys. A **729** 3 (2003)
[35] J. Dilling *et al.*, Int. J. Mass Spectrom. **251** 198 (2006)
[36] M. Smith *et al.*, Phys. Rev. Lett. **101** 202501 (2008)